

Figure S1. SLP-76 RK SH2 mutant impairs contact stability but is dispensable for calcium influx, PLC γ phosphorylation, and ERK1 activation. **(A)** SLP-76 deficient (J14) cells expressing WT human SLP-76.YFP or the SLP-76.RK.YFP SH2 mutant chimera were stimulated and imaged as in Figure 1. Kymographs depict movement within regions that encompass the entirety of the cell diameter over time (20 μ m x 180 s). The contours of the cell contact are outlined in white and illustrate our scoring criteria for the “Stable” and “Fluctuating” cells tallied in Fig. 1E. **(B)** J14 cells expressing mYFP, WT SLP76, or a SH2 mutant SLP-76 were stimulated or imaged as above. Diagram indicates a time course representation of our boundary fluctuation quantification algorithm described in Ophir *et al* 2013. Briefly, areas of boundary growth are marked in blue, while areas of boundary contraction are marked in red. Boundary fluctuation was calculated in Fig. 1F by dividing the areas of red or blue fluctuation over the total cell area during the length of the movie. **(C)** J14 cells transiently expressing mYFP chimeras were assayed for TCR-induced Ca²⁺ entry (n=3 experiments). All errors are displayed as SEMs; p-values indicate significant differences from J14 cells expressing wild-type SLP-76.YFP (Student's two-tailed t-test for unpaired samples: *, p < 0.05; ** p < 0.01). **(D)** SLP-76 deficient J14 cells were lentivirally transduced with either WT SLP-76 or the SLP-76 RK SH2 mutant. Parental J14 and transduced cells were either left unstimulated or stimulated with C305 for 2 min, 5 min, or 10 min. Total lysates were western blotted as indicated (n=2 experiments).

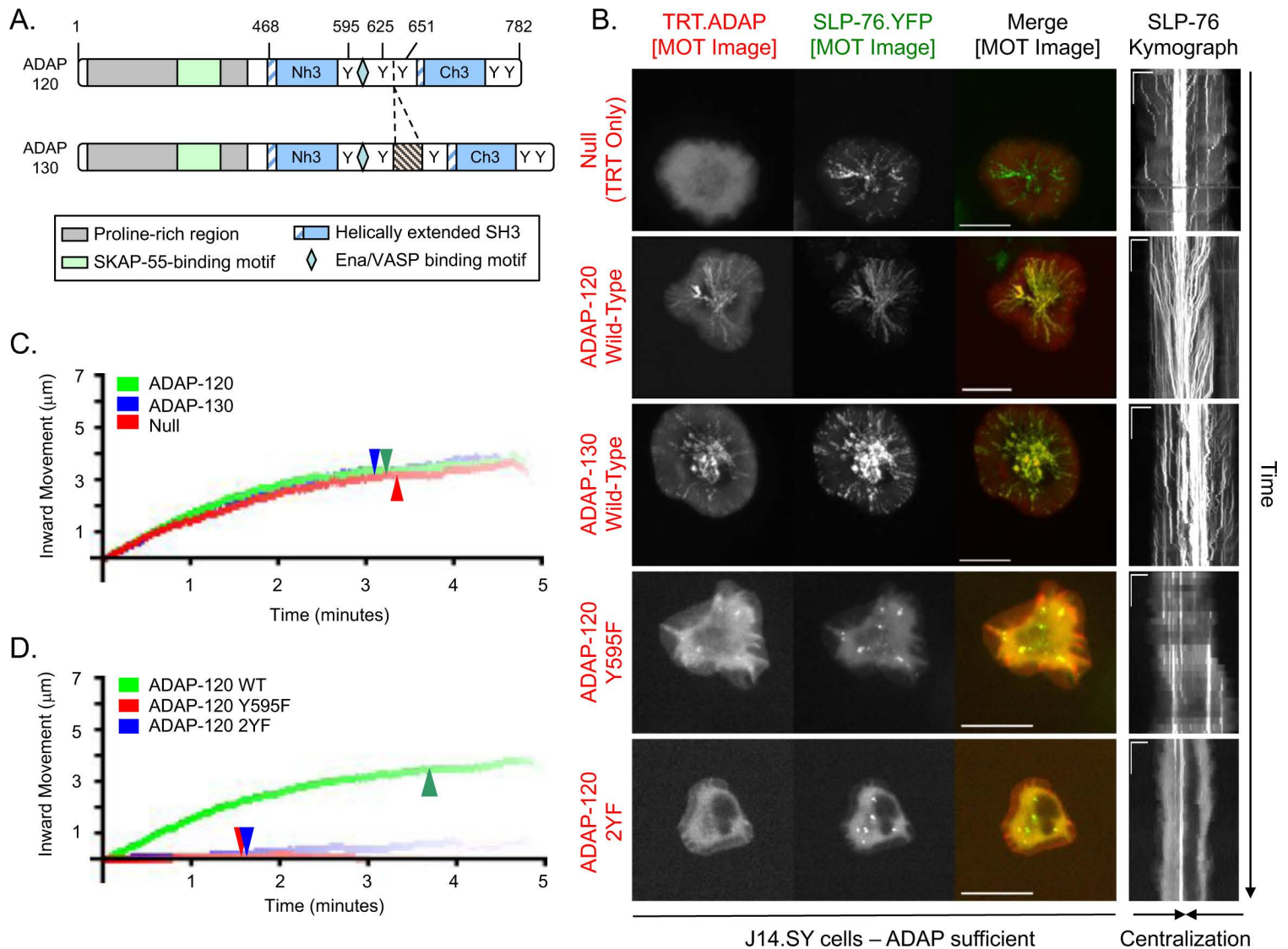


Figure S2. ADAP splice variants are recruited into persistent microclusters by SLP-76.

(A) Domain structures of ADAP splice variants. For a diagram of the ADAP Y595F and 2YF tyrosine mutants see Figure 3A. **(B)** J14.SY cells transiently expressing either 3xFlag.TRT or the indicated 3xFlag.TRT.ADAP chimeras were stimulated and imaged as in Figure 1. MOT images were prepared from movies of SLP-76.YFP (green in merge) and 3xFlag.TRT (red in merge); kymographs were prepared from movies of SLP-76.YFP (see Figure 1 for descriptions of MOTs and kymographs). Scale bars are as in Figure 1B. **(C-D)** Composite kymographs depict average SLP-76 microcluster properties for conditions shown in (B), above. Microcluster properties, number of experiments, number of cells analyzed, and statistical comparisons are listed in Table S2.

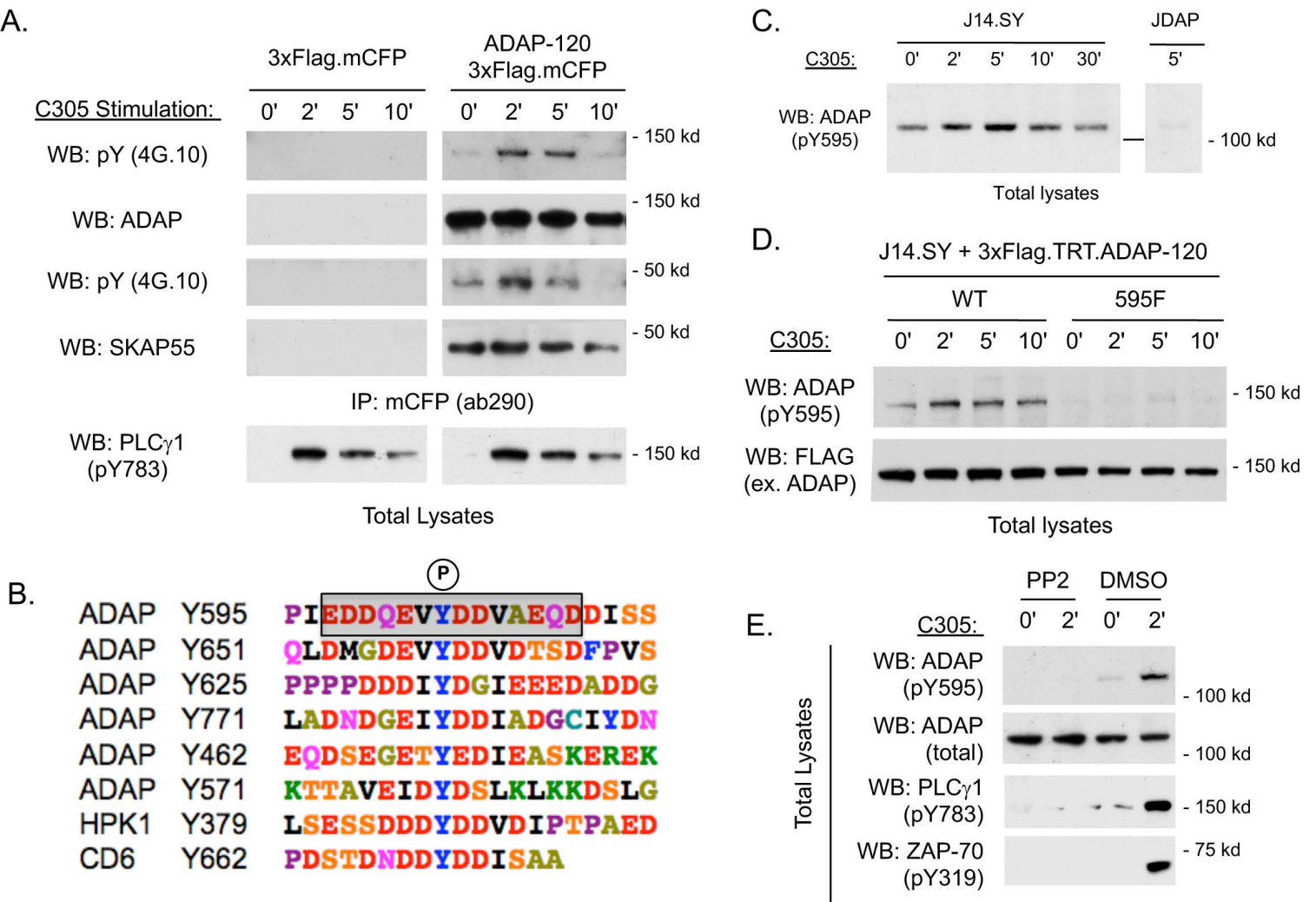
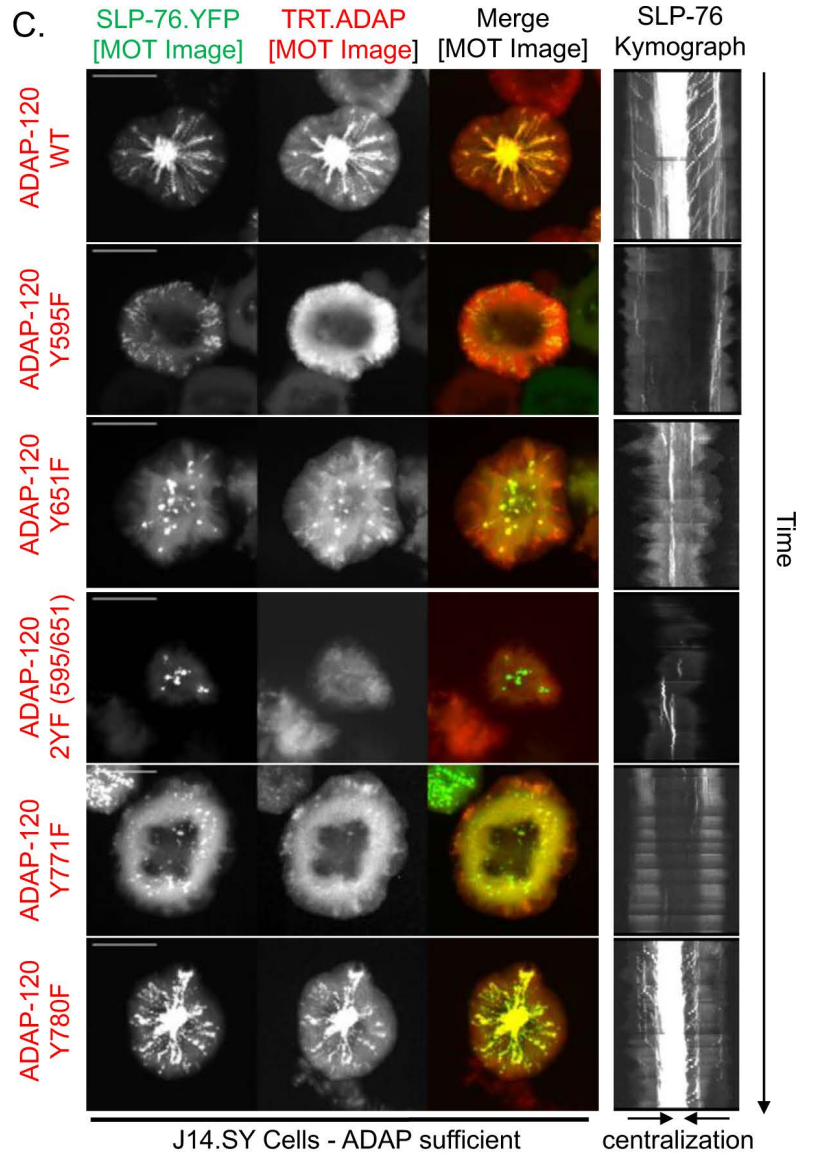
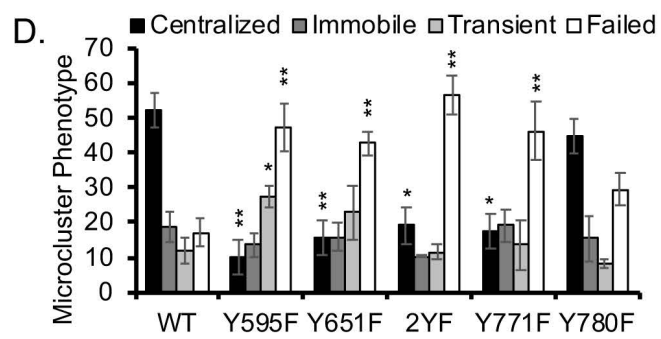
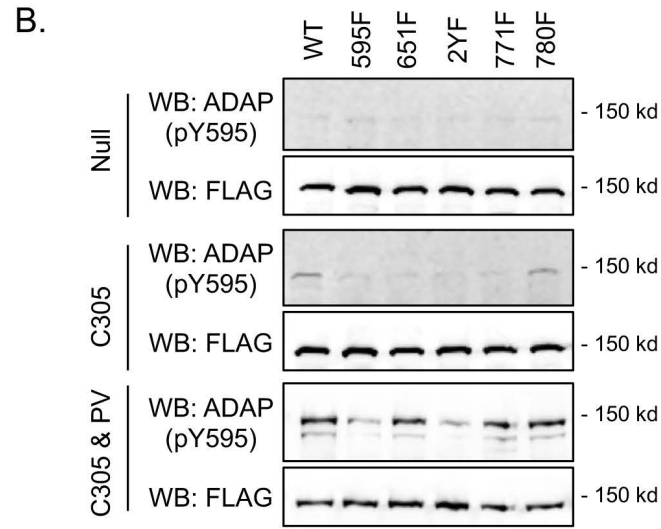
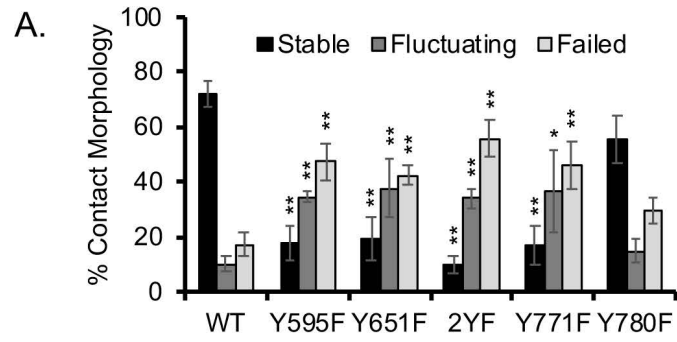


Figure S3. Validation of anti-ADAP pY595 antibody. (A) JDAP cells were transiently reconstituted with ADAP-120.3xFlag.mCFP, stimulated, and lysed. Exogenous ADAP was immunoprecipitated with anti-CFP (ab290) and western blotted as indicated. pY783 PLC γ 1 provides a control for TCR activation. (B) Alignments of putative SLP-76 SH2 domain-binding sites in *Homo sapiens* ADAP-120, HPK1, and CD6. Antisera targeting ADAP pY595 were raised in rabbits and affinity purified using the boxed phosphopeptide. (C) To evaluate the kinetics of ADAP pY595 phosphorylation, J14.SY and JDAP cells were stimulated with C305 and western blotted for ADAP pY595. (D) J14.SY cells stably expressing either 3xFlag.TRT.ADAP-120.WT or 3xFlag.TRT.ADAP-120.595F chimeras were stimulated with C305, lysed, and western blotted for ADAP pY595. FLAG blot demonstrates even expression of the exogenous construct. (E) J14.SY cells were pre-treated with 10 μ M PP2 or with DMSO carrier for 10 min prior to stimulation with C305. Total lysates were blotted as indicated (n=2). pY319 ZAP-70 and pY783 PLC γ 1 provide controls for TCR activation. All western blots are representative of two or more independent experiments.



E.

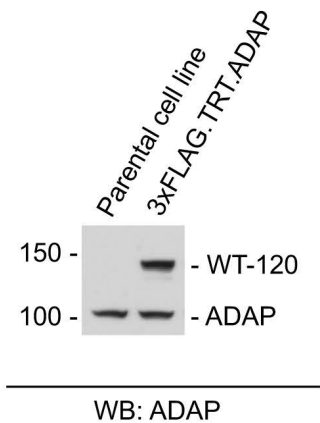
ADAP Chimera	Replicates	
	cells	wells
WT ADAP	246	8
Y595F	152	3
Y651	160	3
2YF	79	2
Y771F	130	3
Y780F	213	5

ADAP Chimera	Contact Morphology					
	Stable		Fluctuating		Failed	
	Mean +/- SEM	p vs. WT	Mean +/- SEM	p vs. WT	Mean +/- SEM	p vs. WT
WT ADAP	72.2 ± 5.0	1.00000	10.4 ± 3.1	1.00000	17.4 ± 4.2	1.00000
Y595F	18.1 ± 6.4	0.00012	34.5 ± 1.9	0.00087	47.4 ± 6.8	0.00250
Y651	19.5 ± 8.0	0.00018	37.9 ± 10.4	0.00280	42.6 ± 3.5	0.00469
2YF	10.0 ± 3.0	0.00022	34.1 ± 3.5	0.00463	55.9 ± 6.6	0.00172
Y771F	17.1 ± 6.9	0.00011	36.7 ± 15.2	0.01213	46.2 ± 8.5	0.00424
Y780F	55.5 ± 8.5	0.07145	15.1 ± 4.4	0.34950	29.5 ± 4.8	0.06950

ADAP Chimera	Microcluster Phenotype									
	Central		Immobile		Erratic		Transient		Failed	
	Mean +/- SEM	p vs. WT	Mean +/- SEM	p vs. WT	Mean +/- SEM	p vs. WT	Mean +/- SEM	p vs. WT	Mean +/- SEM	p vs. WT
WT ADAP	51.9 ± 6.8	1.00000	18.7 ± 4.3	1.00000	0.3 ± 0.3	1.00000	12.0 ± 3.8	1.00000	17.1 ± 4.0	1.00000
Y595F	10.3 ± 1.6	0.00372	13.5 ± 3.6	0.47429	1.5 ± 1.0	0.09564	27.4 ± 2.8	0.03465	47.4 ± 6.8	0.00198
Y651	15.7 ± 1.9	0.00823	15.9 ± 3.9	0.70231	3.0 ± 2.7	0.07073	22.8 ± 7.6	0.15605	42.6 ± 3.5	0.00365
2YF	19.1 ± 8.4	0.04059	10.3 ± 0.4	0.34625	2.6 ± 0.1	0.00330	11.6 ± 2.2	0.95443	56.5 ± 5.7	0.00118
Y771F	17.3 ± 5.6	0.01186	19.1 ± 4.8	0.95749	3.8 ± 3.5	0.05767	13.5 ± 7.3	0.83363	46.2 ± 8.5	0.00345
Y780F	44.5 ± 1.8	0.38813	15.4 ± 6.5	0.64533	2.4 ± 1.7	0.10586	8.2 ± 1.4	0.43563	29.5 ± 4.8	0.05822

Figure S4: ADAP tyrosines 595, 651, and 771 are essential and are functionally equivalent. J14.SY cells were stably transduced with the indicated 3xFlag.TRT.ADAP-120 chimeras. **(A)** Cells were visualized for 5 minutes while responding to OKT3-coated glass surfaces. Contact formation and morphology were manually scored for all ADAP-expressing cells in the imaging field. **(B)** Transduced cells were left unstimulated, stimulated with C305 for 2 minutes, or stimulated with C305 and pervanadate for 10 minutes. Total lysates were western blotted as indicated. **(C)** Image stacks captured in (A) were used to generate maximum over time (MOT) images and kymographs spanning the entire imaging period **(D)** Microcluster phenotypes were manually scored for all cells imaged in (A). **(E)** Data, errors, numbers of independent wells, and p-values for panels (A) and (D). All errors are displayed as SEM of independent wells; p-values indicate significant differences from J14.SY cells expressing wild-type ADAP-120 (Student's two-tailed t-test for unpaired samples: *, $p < 0.05$; ** $p < 0.01$).

A.



B.

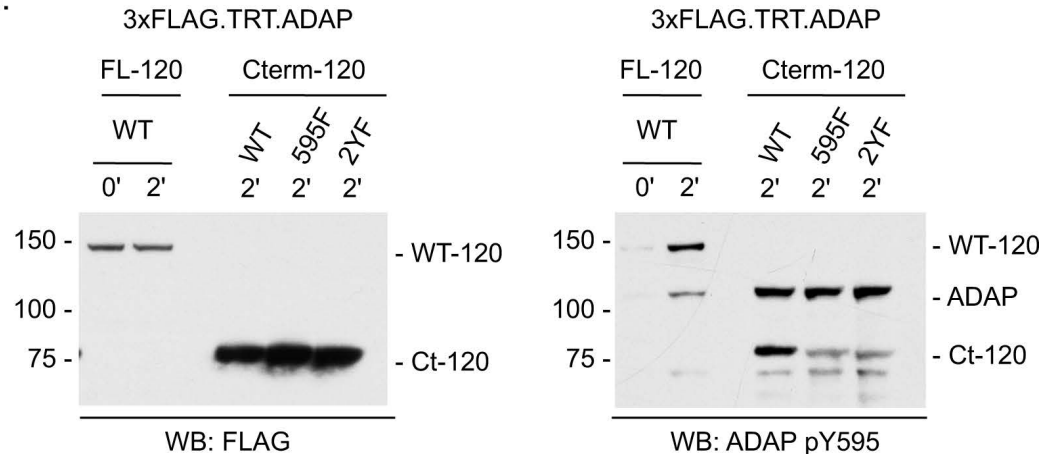


Figure S5. ADAP C-terminal tyrosine mutants do not support Y595 phosphorylation following TCR ligation.

J14.SY cells were stably transduced with the wild-type 3xFlag.TRT.ADAP-120 chimera or with the indicated C-terminal chimeras. Lines expressing exogenous wild-type ADAP were sorted to obtain near-endogenous levels of protein, while the C-terminal lines were sorted for levels approximately 25-fold in excess of the endogenous protein. Cells were left unstimulated or stimulated for 2 minutes with C305; total lysates were analyzed by western blotting. **(A)** Total ADAP blots confirm that exogenous ADAP-120 (WT-120) is expressed at near-endogenous (ADAP) levels. **(B)** In conjunction with (A), anti-FLAG (left) and anti-ADAP pY595 (right) blots demonstrate that the wild-type C-terminal fragment (Ct-120) and endogenous ADAP are comparably phosphorylated despite the overexpression of this fragment relative to endogenous ADAP. All western blots are representative of three or more independent experiments.

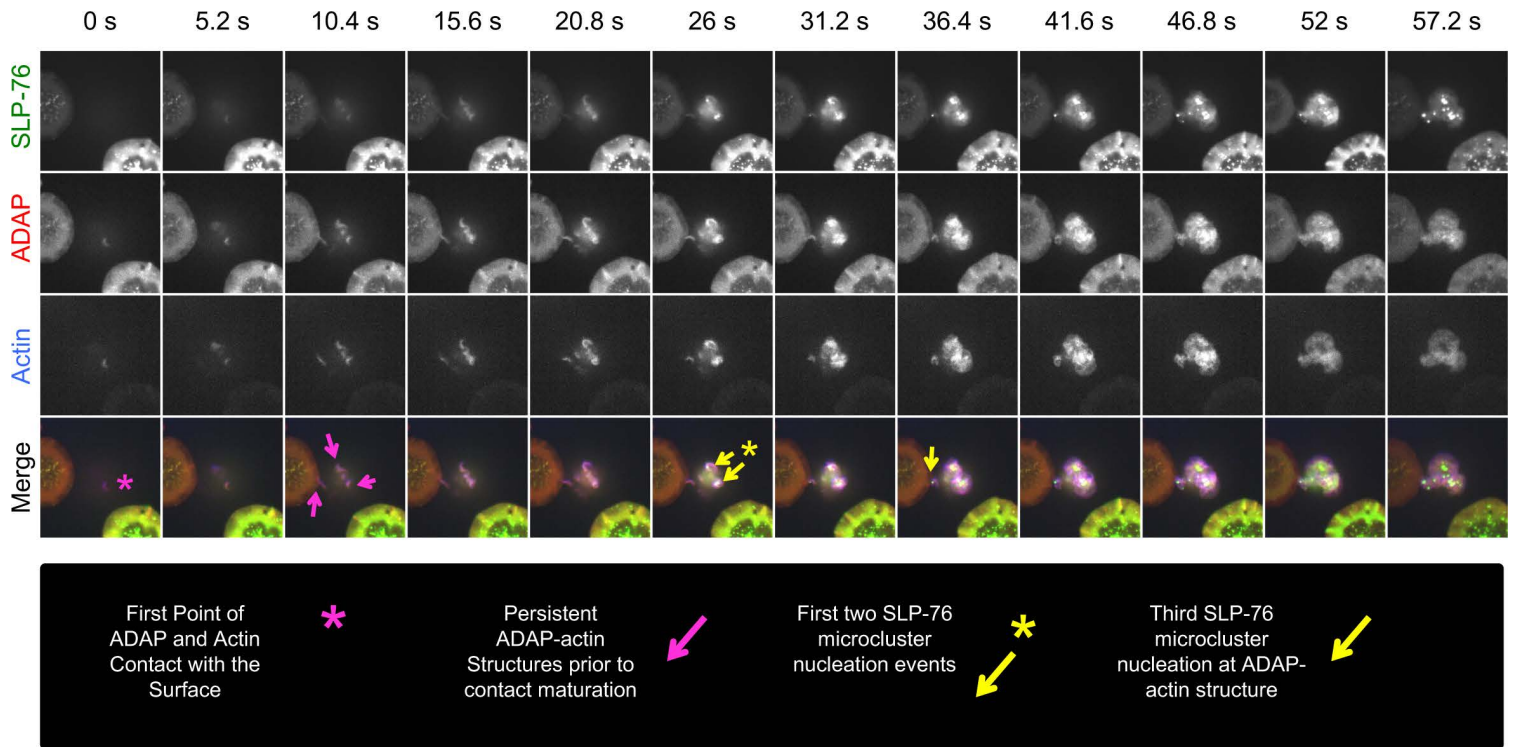


Figure S6: SLP-76 microclusters nucleate from ADAP and actin-enriched protrusions

during T cell contact formation. J14.SY cells expressing 3xFlag.TRT.ADAP-120 were transiently transfected with mCFP.β-actin. The cells were stimulated and imaged as described in Figure 2. Representative images depict the first minute of cellular contact. Magenta arrowheads identify three different ADAP and actin-rich protrusive structures contacting the substrate. Yellow arrows emphasize subsequent SLP-76 microcluster formation on these cytoskeletal structures, with the yellow asterisks indicating the first microcluster nucleation events (n=2 experiments, 12 TRT.ADAP⁺ mCFP-β-actin⁺ J14.SY cells captured during contact formation).

Table S1. The SLP-76 SH2 domain contributes to SLP-76 microcluster persistence and movement.

SLP-76 chimeras	Persistence (s)	p vs. WT	Movement (μm)	p vs. WT	Max Speed (nm s^{-1})	p vs. WT	% SLP-76 in clusters	p vs. WT	<i>n</i> (exp)	<i>n</i> (cell)
SLP-76.WT <i>Hs</i>	218.9 \pm 7.1	n.a.	4.05 \pm 0.28	n.a.	116.9 \pm 7.0	n.a.	57.1 \pm 2.7	n.a.	6	46
SLP-76.RK <i>Hs</i>	131.7 \pm 24.4	6.4e-3	0.56 \pm 0.04	1.7e-7	55.1 \pm 3.9	1.6e-5	8.8 \pm 2.0	5.6e-8	6	45

<i>Mm</i> vs. matched <i>Hs</i>	Persistence (s)	p vs. <i>Hs</i>	Movement (μm)	p vs. <i>Hs</i>	Max Speed (nm s^{-1})	p vs. <i>Hs</i>	% SLP-76 in clusters	p vs. <i>Hs</i>	<i>n</i> (exp)	<i>n</i> (cell)
SLP-76.WT <i>Mm</i>	200.4 \pm 13.3	0.22	3.77 \pm 0.44	0.59	116.7 \pm 8.9	0.98	48.5 \pm 5.1	0.14	3	19
SLP-76.RK <i>Mm</i>	109.9 \pm 8.6	0.56	0.52 \pm 0.03	0.51	43.8 \pm 1.1	0.09	11.5 \pm 1.5	0.41	3	14

(Upper) J14 cells were transfected with SLP-76.WT or SLP-76.RK (see Figure 1). SLP-76 microcluster behavior was calculated from traces of individual microclusters from cells across the indicated number of experiments. Microcluster properties are shown \pm SEM, based on the number of experiments; p values were calculated using a two-tailed Student's t-test for unpaired samples; significant differences from WT are shaded and in bold. **(Lower)** J14 cells were transfected with murine SLP-76.WT or SLP-76.RK. Microcluster behavior was calculated from traces of individual microclusters from cells across the indicated number of experiments. Microcluster properties are shown \pm SEM, based on the number of experiments; p values were calculated versus the corresponding human chimeras using a two-tailed Student's t-test for unpaired samples; no significant differences were observed.

Table S2. ADAP is required for optimal SLP-76 microcluster movement and persistence.

ADAP chimeras	Persistence (s)	p vs. WT	p vs. TRT	Movement (μm)	p vs. WT	p vs. TRT	Max Speed (nm s^{-1})	p vs. WT	p vs. TRT	% SLP-76 in clusters	p vs. WT	p vs. TRT	n (exp)	n (cell)
TRT control	195.3 \pm 10.0	0.87	n.a.	4.04 \pm 0.35	0.76	n.a.	130.0 \pm 6.5	0.91	n.a.	56.2 \pm 2.7	8.6e-4	n.a.	7	30
120.WT	197.4 \pm 7.3	n.a.	0.87	4.17 \pm 0.21	n.a.	0.76	131.2 \pm 6.9	n.a.	0.91	68.1 \pm 1.5	n.a.	8.6e-4	15	69
130.WT	173.2 \pm 12.4	0.18	0.25	3.48 \pm 0.45	0.20	0.39	120.4 \pm 12.5	0.52	0.49	62.7 \pm 8.6	0.28	0.39	3	15
ADAP-KD	83.4 \pm 12.5	6.7e-6	4.1e-4	0.94 \pm 0.02	5.6e-6	7.8e-4	61.5 \pm 2.5	4.2e-4	3.0e-4	34.7 \pm 4.2	1.9e-7	3.7e-3	3	36
ADAP-KD/AB	196.9 \pm 6.0	0.97	0.92	4.49 \pm 0.30	0.53	0.47	139.6 \pm 9.0	0.61	0.44	71.8 \pm 3.2	0.33	0.013	3	30
120.Y595F	137.8 \pm 14.4	1.6e-3	0.011	0.80 \pm 0.18	4.6e-7	1.7e-4	53.2 \pm 6.9	3.2e-5	7.3e-5	29.6 \pm 7.7	2.9e-7	5.6e-3	4	29
120.2YF	113.7 \pm 9.3	3.5e-5	7.3e-4	0.60 \pm 0.09	1.7e-7	8.8e-5	52.9 \pm 5.5	2.8e-5	4.8e-5	19.6 \pm 3.1	5.4e-11	3.1e-5	4	25
120.Ct-WT	126.6 \pm 9.6	7.4e-5	1.1e-3	0.99 \pm 0.04	1.1e-7	4.4e-5	65.1 \pm 2.6	3.7e-5	2.1e-5	42.6 \pm 4.5	1.5e-6	0.027	5	47
120.Ct-595F	157.9 \pm 9.6	0.034	0.064	3.15 \pm 0.28	0.058	0.17	108.5 \pm 10.5	0.18	0.12	45.9 \pm 5.8	6.5e-5	0.11	3	12
120.Ct-2YF	169.6 \pm 6.4	0.12	0.16	3.58 \pm 0.28	0.26	0.45	135.7 \pm 7.8	0.78	0.64	54.4 \pm 1.9	1.4e-3	0.69	3	21
120.Ct-3YF	193.8 \pm 3.4	0.83	0.93	4.18 \pm 0.33	0.98	0.82	127.8 \pm 15.2	0.84	0.88	61.9 \pm 2.7	0.11	0.25	3	15

J14.SY cells were transfected with the indicated TRT expression vectors (see Figures 2, S2, and 5). SLP-76 microcluster behavior was calculated from traces of individual microclusters from cells across the indicated number of experiments. Microcluster properties are shown \pm SEM, based on the number of experiments; p values were calculated using a two-tailed Student's t-test for unpaired samples; significant differences from wild-type ADAP-120 are shaded light orange and in bold; significant differences from the TRT control are shaded light purple and in bold.

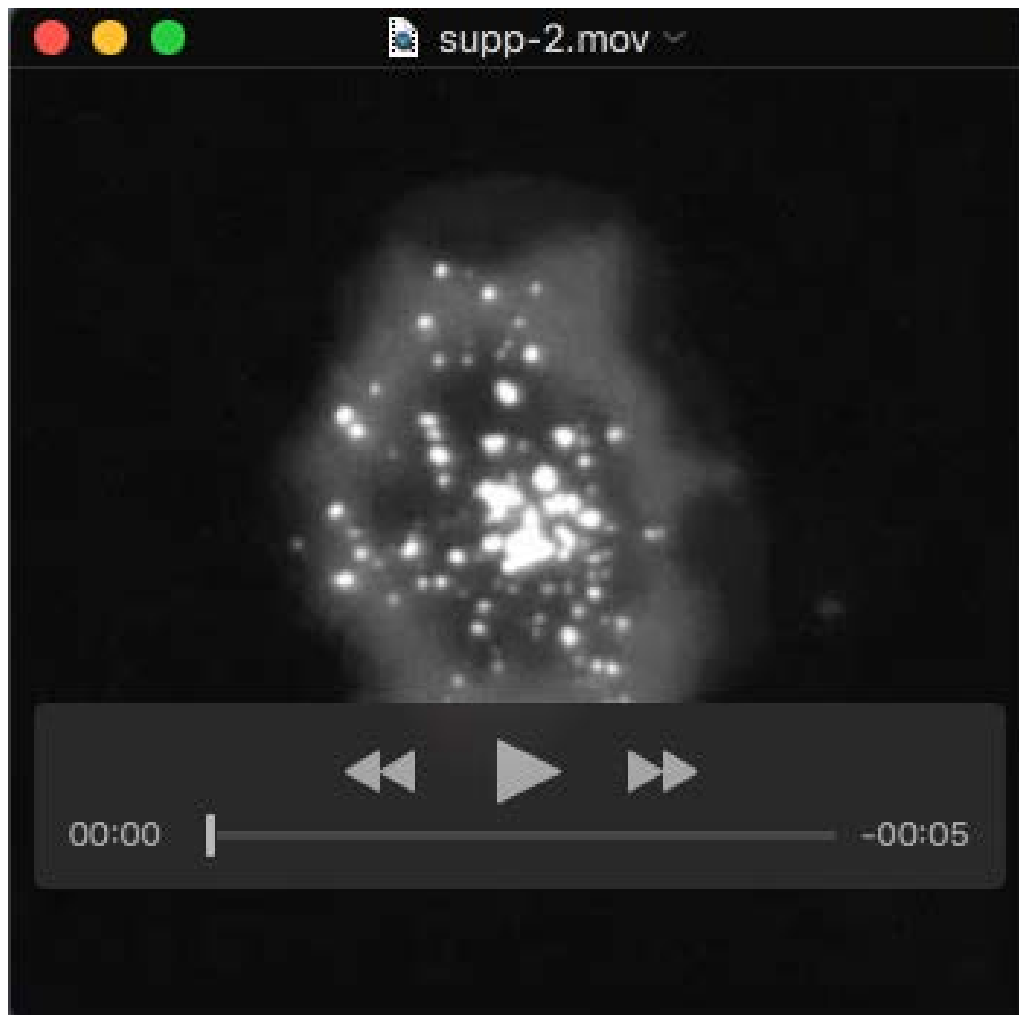
Table S3. ADAP requires both Y595 and Y651 to stabilize SLP-76 microclusters.

ADAP chimeras	Persistence (s)	p vs. WT	p vs. TRT	Movement (μ m)	p vs. WT	p vs. TRT	% SLP-76 in clusters	p vs. WT	p vs. TRT	n (exp)	n (cell)
TRT control	70.0 \pm 8.4	0.001	n.a.	7.8 \pm 2.5	0.015	n.a.	21.7 \pm 9.9	0.012	n.a.	3	15
120.WT	185.6 \pm 13.3	n.a.	0.001	34.7 \pm 6.0	n.a.	0.015	65.5 \pm 6.6	n.a.	0.012	4	22
120.Y595F	112.3 \pm 12.2	0.011	0.046	4.9 \pm 0.2	0.008	0.31	20.2 \pm 4.3	0.004	0.90	3	15
120.2YF	106.2 \pm 3.6	0.004	0.017	9.0 \pm 1.0	0.015	0.69	29.3 \pm 6.3	0.012	0.55	3	15
120.3YF	83.7 \pm 5.0	0.002	0.24	5.7 \pm 1.1	0.009	0.48	24.0 \pm 11.3	0.02	0.89	3	17

JDAP cells were co-transfected with SLP-76 and the indicated TRT expression vectors (see Figure 3). SLP-76 microcluster behavior was calculated from traces of individual microclusters from cells across the indicated number of experiments. Microcluster properties are shown \pm SEM, based on the number of experiments; p values were calculated using a two-tailed Student's t-test for unpaired samples; significant differences from wild-type ADAP-120 are shaded light orange and in bold; significant differences from the TRT control are shaded light purple and in bold.

SUPPLEMENTAL MOVIES.

All movies play back at 60x normal speed. All of the following movies are of cells that were stimulated on OKT3-coated cover slips and imaged continuously for 5 minutes.



Movie S1. The SLP-76 SH2 domain regulates TCR-induced SLP-76 microcluster centralization and persistence (WT SLP-76 movie). SLP-76 deficient Jurkat T cells (J14 cells) were transiently transfected with an expression vector for a wild-type (WT) SLP-76.YFP chimera of human origin.



Movie S2. The SLP-76 SH2 domain regulates TCR-induced SLP-76 microcluster centralization and persistence (RK SLP-76 movie). SLP-76 deficient Jurkat T cells (J14 cells) were transiently transfected with an expression vector for an SH2 mutant (R448K; RK) SLP-76.YFP chimera of human origin.

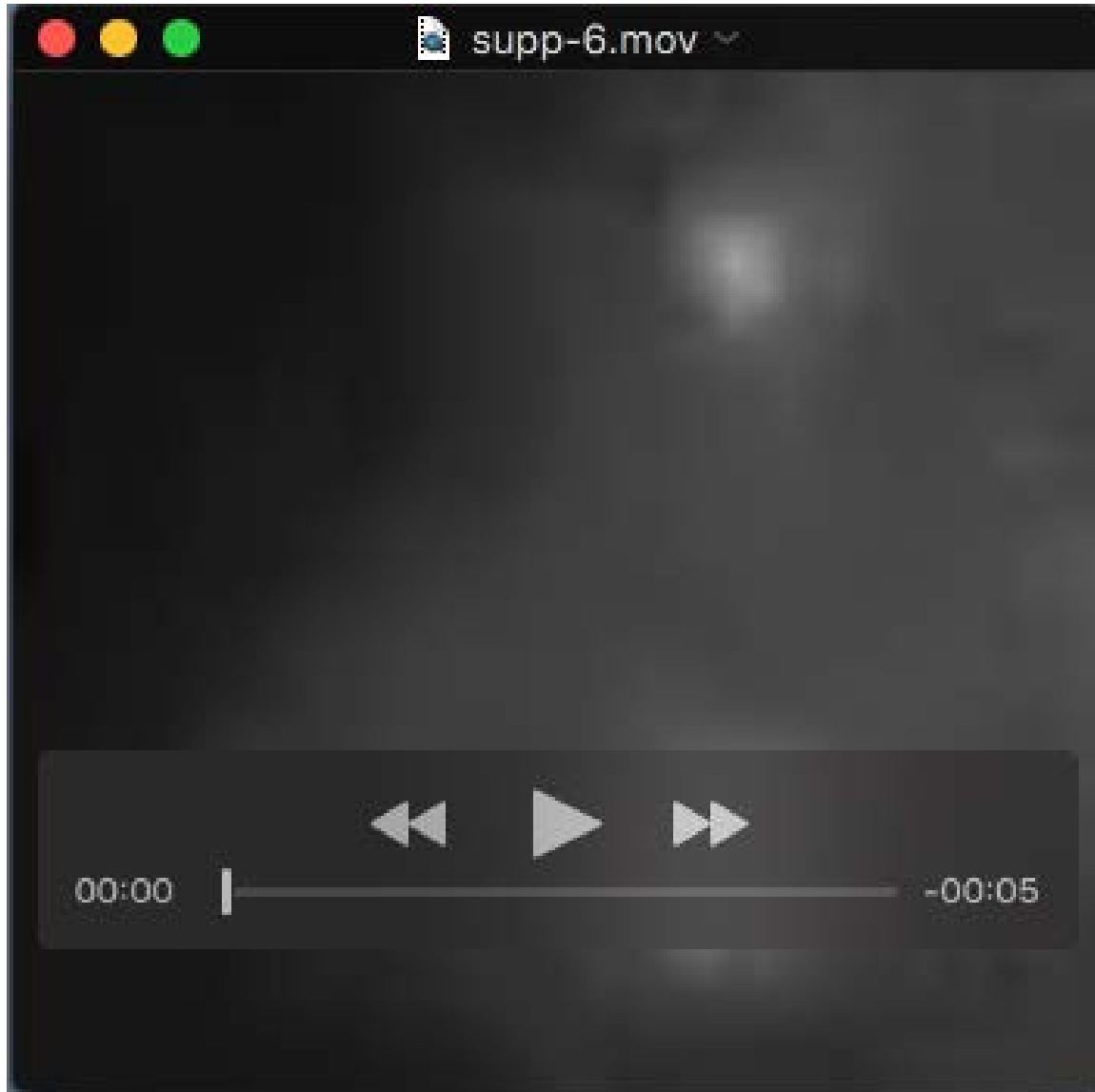


Movie S3. The SLP-76 SH2 domain enables microcluster cohesion (WT STD movie #1).

SLP-76 deficient Jurkat T cells (J14 cells) were transiently transfected with an expression vector for a wild-type (WT) SLP-76.YFP chimera of human origin. Magnification is 3x greater than in movies S1-2.



Movie S4. The SLP-76 SH2 domain enables microcluster cohesion (WT STD movie #2). SLP-76 deficient Jurkat T cells (J14 cells) were transiently transfected with an expression vector for a wild-type (WT) SLP-76.YFP chimera of human origin. Magnification is 3x greater than in movies S1-2.



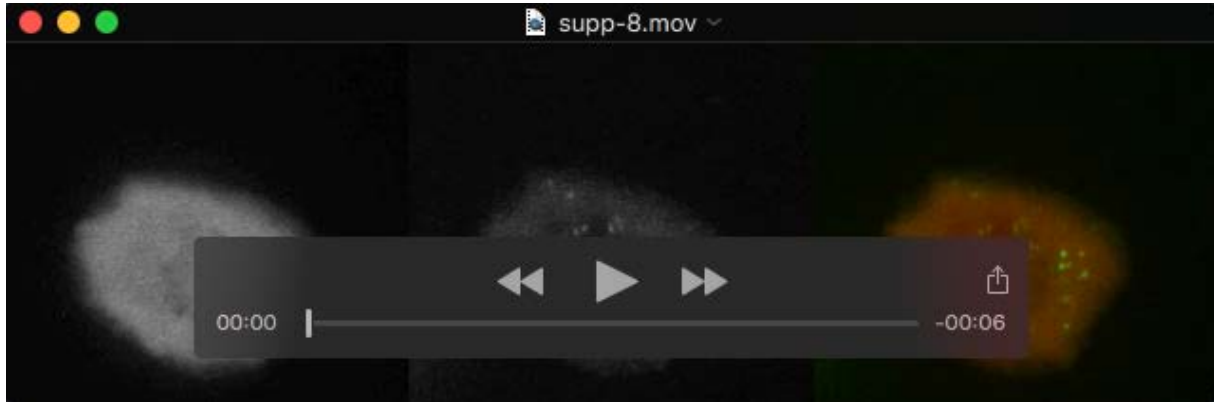
Movie S5. The SLP-76 SH2 domain enables microcluster cohesion (RK STD movie #1).

SLP-76 deficient Jurkat T cells (J14 cells) were transiently transfected with an expression vector for an SH2 mutant (R448K; RK) SLP-76.YFP chimera of human origin. Magnification is 3x greater than in movies S1-2.



Movie S6. The SLP-76 SH2 domain enables microcluster cohesion (RK STD movie #2).

SLP-76 deficient Jurkat T cells (J14 cells) were transiently transfected with an expression vector for an SH2 mutant (R448K; RK) SLP-76.YFP chimera of human origin. Magnification is 3x greater than in movies S1-2.



Movie S7. The ADAP-120 and ADAP-130 isoforms both enter TCR-induced SLP-76 microclusters and lamellipodia (TRT control movie). J14.SY cells were transiently transfected with a 3xFlag.TRT control for the ADAP expression vectors seen in movies S8-S9. TRT protein is shown in the left panel and in red in the merge, SLP-76 in the middle panel and in green in the merge.



Movie S8. The ADAP-120 and ADAP-130 isoforms both enter TCR-induced SLP-76 microclusters and lamellipodia (ADAP-120 movie). J14.SY cells were transiently transfected with a 3xFlag.TRT.ADAP expression vector for ADAP-120. ADAP is shown in the left panel and in red in the merge, SLP-76 in the middle panel and in green in the merge.



Movie S9. The ADAP-120 and ADAP-130 isoforms both enter TCR-induced SLP-76 microclusters and lamellipodia (ADAP-130 movie). J14.SY cells were transiently transfected with a 3xFlag.TRT.ADAP expression vector for ADAP-130. ADAP is shown in the left panel and in red in the merge, SLP-76 in the middle panel and in green in the merge.



Movie S10. ADAP enhances the persistence and movement of TCR-induced SLP-76 microclusters (ADAP KD movie). J14.SY cells were transiently transfected with a dual expression vector encoding an shRNA specific for the 3'UTR of ADAP and a 3xFlag.TRT marker (ADAP KD). TRT protein is shown in the left panel and in red in the merge, SLP-76 in the middle panel and in green in the merge.



Movie S11. ADAP enhances the persistence and movement of TCR-induced SLP-76 microclusters (ADAP KD/AB movie). J14.SY cells were transiently transfected with a dual expression vector encoding an shRNA specific for the 3'UTR of ADAP and a 3xFlag.TRT.ADAP-120 chimera (ADAP KD/AB). ADAP was expressed at near endogenous levels, as confirmed in Figure 2A. ADAP is shown in the left panel and in red in the merge, SLP-76 in the middle panel and in green in the merge.



Movie S12. The overexpressed C-terminal fragment of ADAP antagonizes SLP-76 microcluster persistence and movement via phosphotyrosine-dependent interactions (WT C-term movie). J14.SY cells were transiently transfected with an expression vector encoding a 3xFlag.TRT-tagged chimera of the wild-type C-terminal fragment of ADAP-120. ADAP is shown in the left panel and in red in the merge, SLP-76 in the middle panel and in green in the merge.



Movie S13. The overexpressed C-terminal fragment of ADAP antagonizes SLP-76 microcluster persistence and movement via phosphotyrosine-dependent interactions.

(Y595F C-term movie) J14.SY cells were transiently transfected with an expression vector encoding a 3xFlag.TRT-tagged chimera of the Y595F mutated C-terminal fragment of ADAP-120. ADAP is shown in the left panel and in red in the merge, SLP-76 in the middle panel and in green in the merge.



Movie S14. ADAP enters cytoskeletal contact structures prior to the recruitment of SLP-76. J14.SY cells were transiently transfected with ADAP knockdown-addback vectors as in movies S10-11. A representative cell was captured during its first moments of contact with the stimulatory cover slip. ADAP is shown in the left panel and in red in the merge, SLP-76 in the middle panel and in green in the merge. Note that ADAP is enriched in protrusive structures before SLP-76 is recruited into the contact, that SLP-76 microclusters form at the tips of these projections, and that ADAP enters the nascent microclusters concurrently with SLP-76.



Movie S15. The SLP-76 SH2 domain is dispensable for the transient enrichment of ADAP into contact structures (TRT.ADAP with mYFP). J14 cells were transiently co-transfected with 3xFlag.TRT.ADAP-120.WT and mYFP expression vectors. ADAP is shown in the left panel and in red in the merge, mYFP in the middle panel and in green in the merge.



Movie S16. The SLP-76 SH2 domain is dispensable for the transient enrichment of ADAP into contact structures (TRT.ADAP with SLP-76.WT.mYFP). J14 cells were transiently co-transfected with 3xFlag.TRT.ADAP-120.WT and SLP-76.WT.mYFP expression vectors. ADAP is shown in the left panel and in red in the merge, mYFP in the middle panel and in green in the merge.



Movie S17. The SLP-76 SH2 domain is dispensable for the transient enrichment of ADAP into contact structures (TRT.ADAP with SLP-76.RK.mYFP). J14 cells were transiently co-transfected with 3xFlag.TRT.ADAP-120.WT and SLP-76.RK.mYFP expression vectors. ADAP is shown in the left panel and in red in the merge, SLP-76 in the middle panel and in green in the merge. Note that ADAP is enriched in the lamellipodia formed in the presence of the SH2 domain-mutated SLP-76 chimera. ADAP also forms labile 'patches' in the absence of a functional SLP-76 SH2 domain.